Water Science & Technology

Water Science & Technology Vol 85 No 1, 535 doi: 10.2166/wst.2021.617

Photocatalytic ozonation in an immersion rotary body reactor for the removal of micro-pollutants from the effluent of wastewater treatment plants

Simon Mehling [a,*], Tobias Schnabel[b] and Jörg Londong[a]

[a] Bauhaus-Universität Weimar, Department of Civil Engineering, Professorship of Urban Water Management, Weimar, Germany
[b] MFPA Weimar – Materials Research and Testing Institute Weimar, Weimar, Germany
*Corresponding author. E-mail: simon.theodor.mehling@uni-weimar.de

SM, 0000-0002-9188-2074

ABSTRACT

Carrier-bound titanium dioxide catalysts were used in a photocatalytic ozonation reactor for the degradation of micro-pollutants in real wastewater. A photocatalytic immersion rotary body reactor with a 36-cm disk diameter was used, and was irradiated using UV-A light-emitting diodes. The rotating disks were covered with catalysts based on stainless steel grids coated with titanium dioxide. The dosing of ozone was carried out through the liquid phase via an external enrichment and a supply system transverse to the flow direction. The influence of irradiation power and ozone dose on the degradation rate for photocatalytic ozonation was investigated. In addition, the performance of the individual processes photocatalysis and ozonation were studied. The degradation kinetics of the parent compounds were determined using liquid chromatography tandem mass spectrometry. First-order kinetics were determined for photocatalysis and photocatalytic ozonation. A maximum reaction rate of the reactor was determined, which could be achieved by both photocatalysis and photocatalytic ozonation. At a dosage of 0.4 mg O_3/mg DOC, the maximum reaction rate could be achieved using 75% of the irradiation power used for sole photocatalysis, allowing increases in the energetic efficiency of photocatalytic wastewater treatment processes. The process of photocatalytic ozonation is suitable to remove a wide spectrum of micro-pollutants from wastewater.

Key words: anthropogenic micro-pollutants, photocatalysis, photocatalytic ozonation, titan dioxide, UV-A light, wastewater treatment

HIGHLIGHT

- Within the work, reaction rates for the degradation of micro-pollutants in real wastewater matrix are presented. due to the number of investigated pollutants as well as the practical investigation conditions, a more precise evaluation of the use of photocatalysis and photocatalytic ozonation for wastewater treatment is possible.

GRAPHICAL ABSTRACT

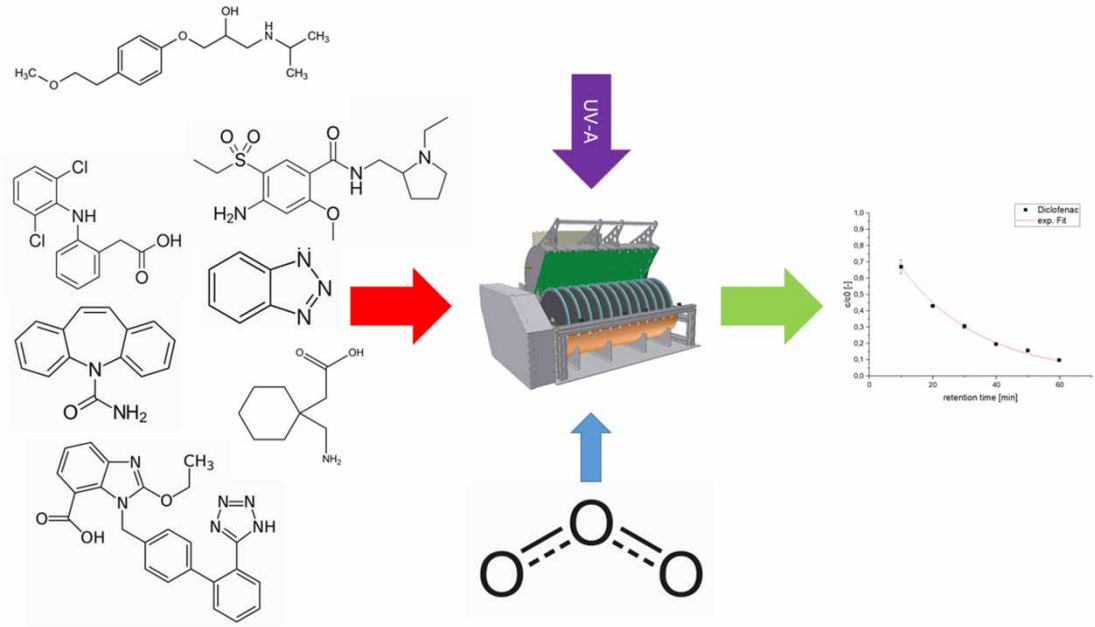

INTRODUCTION

Through advances in the field of instrumental analysis, the input and behavior of the lowest concentrations of chemicals in the environment have been made measurable. It has been demonstrated that anthropogenically formed substances cause adverse changes, especially in aquatic ecosystems, even at the lowest concentration ranges, with wastewater being one of the main input pathways (Weber *et al.* 2014; Aemig *et al.* 2021). Such micro-pollutants are only partially degraded or separated by conventional wastewater treatment methods (Abegglen & Siegrist 2012; Kanaujiya *et al.* 2019). Based on this problem, methods of advanced wastewater treatment (fourth treatment stage) have been developed. Adsorptive processes using powdered or granulated activated carbon and oxidative processes using ozone have been implemented on an industrial scale in many projects (Bourgin *et al.* 2018; Guillossou *et al.* 2019; Guillossou *et al.* 2020). Advanced oxidation processes (AOPs), which enable the oxidation of wastewater constituents by reactants such as hydroxyl radicals, superoxides, ozonides and electrode defects at ambient temperatures, are currently not used in wastewater treatment outside of research projects (Kanakaraju *et al.* 2018). The main advantage of AOPs is the higher oxidation strength of the hydroxyl radicals, which promises a substance-independent high degradation performance up to mineralization (Kisch 2015; Kanakaraju *et al.* 2018). The group of AOPs can be further subdivided manifold times in terms of their mechanisms of action and areas of application, with developmental issues and outcomes continuing to evolve (Garrido-Cardenas *et al.* 2019). Other areas of application can be, for example, the treatment of leachate or the treatment of drinking water (Sillanpää *et al.* 2018; Hassan *et al.* 2021).

Within this work, the AOPs of photocatalysis as well as photocatalytic ozonation are investigated. While in photocatalysis hydroxyl radicals are formed only by the excitation of semiconductor materials by UV-A radiation, in photocatalytic ozonation hydroxyl and other radical species are formed to a higher extent by the combined application of ozone and photoactive semiconductors through synergy effects (Mehrjouei *et al.* 2012). This method has already been studied in different variations by many research groups worldwide (Mehrjouei *et al.* 2015). Studies by many groups (Gimeno *et al.* 2007; Rivas *et al.* 2012; Santiago-Morales *et al.* 2012; Rodríguez *et al.* 2013; Chávez *et al.* 2019; among others), have been carried out related to an application within wastewater treatment.

During the photocatalysis with titanium dioxide, charge separation occurs on the semiconductor by irradiation with UV-A light (320–400 nm). Electron holes and free electrons are formed on the valence band (Equation 1). The formation of hydroxyl radicals via photocatalysis is primarily possible through a pH-dependent reaction of the electron holes with

hydroxide ions or water molecules (Equation 2) (Gaya & Abdullah 2008):

$$TiO_2 + h_\gamma \rightarrow TiO_2(h^+ + e^-) \quad (1)$$

$$h^+ + OH^- \rightarrow OH\cdot \quad (2)$$

In photocatalytic ozonation, additionally ozone molecules adsorbs on the surface of the catalyst, producing superoxide ions (Mehrjouei *et al.* 2015) (Equation 3):

$$O_3 + h^+ \rightarrow \cdot O + O_2 \quad (3)$$

If excited electrons fall back into the electron holes of the valence band, the reaction is finished and thermal energy is released (Mecha & Chollom 2020). This unwanted process is called recombination. If the excited electrons react with acceptors, the recombination rate of electron–hole pairs can be reduced (Mehrjouei *et al.* 2015). Here, photocatalytic ozonation benefits from the higher electron affinity of ozone (2.1 eV) compared to oxygen (0.44 eV) (Pichat *et al.* 2000). Furthermore, hydrogen peroxide formed via various intermediates can also react with excited electrons (Augustina *et al.* 2005). In sum, the following electron–acceptor reactions are possible:

$$O_{2(ads)} + e^- \rightarrow \cdot O_2^- \quad (4)$$

$$O_{3(ads)} + e^- \rightarrow \cdot O_3^- \quad (5)$$

$$H_2O_{2(ads)} + e^- \rightarrow OH\cdot + OH^- \quad (6)$$

Within the oxidation medium, further chain reactions are possible in which among others $OH_2\cdot$, $OH_3\cdot$, $OH_4\cdot$ are formed and consumed (Mehrjouei *et al.* 2015). The oxidation of micro-pollutants takes place primarily through electron–holes, hydroxyl radicals and ozone (Mena *et al.* 2012):

$$pollutant_{(ads)} + h^+ \xrightarrow{multistep} CO_x, NO_x, SO_x, etc \quad (7)$$

$$pollutant_{(ads)} + OH\cdot \xrightarrow{multistep} CO_x, NO_x, SO_x, etc \quad (8)$$

$$pollutant + O_3 \rightarrow [pollutant]^+ + \cdot O_3^- \quad (9)$$

In this work, the degradation of a wide range of pharmaceuticals in real wastewater matrix was investigated. The suitability of a technology as a fourth treatment step for municipal wastewater treatment plants requires the degradation of a wide range of compounds (Abegglen & Siegrist 2012). Eight micro-pollutants were analyzed in a real wastewater matrix within this work. The micro-pollutants investigated allow the assessment of the treatment performance according to the Swiss methodology, which has been applied legally binding since 2016 (GSchV 2020). Here, an 80% degradation of selected indicator substances in proportion to the raw wastewater is required. The tests were carried out on a semi-technical scale using carrier-bound catalyst material. The type of reactor used, the immersion rotary body reactor, represents an adaptation of other photocatalytic processes for wastewater treatment, with the aim of achieving the most practicable, interference-free and low-maintenance operation possible. UV-A light-emitting diodes (LEDs) were used here as the radiation source. Solar photocatalysis or photocatalytic ozonation is also an option. However, this leads to different requirements for catalyst materials (Xiao *et al.* 2020). Within the test series, the influence of the main process parameters irradiation power and ozone dose on the elimination efficiency of this reactor type was investigated. Experiments concerning the degradation of pharmaceuticals via photocatalytic ozonation were carried out by several groups (Aguinaco *et al.* 2012; Rivas *et al.* 2012). However for particulate photocatalytic ozonation there has been no measurement within the real wastewater matrix except for diclofenac available. Kang *et al.* (2021) investigated photocatalytic ozonation within a carrier-bound reactor for phenol within ultrapure water and the real wastewater matrix.

METHODS

Chemicals and materials

The catalyst material used was similar to previous works with more detailed descriptions (Schnabel *et al.* 2020, 2021). The material was coated onto a V4A stainless steel mesh (316 L/1.4404). The mesh size was 200 μm and the wire thickness was 100 μm. The coating was made using a suspension of anatase-modified titanium dioxide nanoparticles of 14 nm diameter. The anatase content of the titanium dioxide was 90% and the Brunauer–Emmett–Teller (BET) surface area of the particles was 50 m^2/g. A 10 μg/l terbutryn solution in methanol was used as an internal standard within the micro-pollutant analysis. The terbutryn was purchased with a purity of 99.5% from Sigma Aldrich. The following substances were used in analytical purity for calibration: amisulpride (Gentham Life Science), benzotriazole (Gentham Life Science), candesartan (BLD Pharma), carbamazepine (Sigma Aldrich), diclofenac (Cayman chemical Company), gabapentin (Gentham Life Science), 1-methylbenzotriazole (Chempure), and metoprolol (Sigma Aldrich). For the measurement of DOC, a calibration line was prepared from aqueous potassium hydrogen phthalate (for analysis) solutions. The potassium hydrogen phthalate was purchased from Sigma Aldrich. A platinum catalyst on ceramic supports from Analytik Jena was used as the catalyst for the thermal oxidation of the analysis.

Experimental set-up and procedure

The experimental unit was located at the Weimar Tiefurt wastewater treatment plant, Germany, and was continuously fed with its effluent. The tests were conducted in December 2020 and January 2021 under dry weather conditions. The experimental plant was composed of two main components: a photocatalytic immersion rotary body reactor and an ozone generation and injection system.

The photocatalytic immersion rotary body reactor consists of 12 rotating discs of 36 cm diameter, which are covered on both sides with catalyst material (Figure 1). This results in a total irradiated catalyst area of 2.44 m^2. The parts of the rotating disks on the air side are uniformly irradiated with adjustable power via UV-A LEDs. On the water side, the reactor is divided into 12 cascades by the arrangement of partitions between each rotating disk, which are flowed through in series. The reactor has a hydraulic volume of 25 liters. Each individual cascade also has an inlet to which the ozonation unit is connected. The ozonation plant consists of the components ozone generator, inlet nozzle and tubular reactor and ozone measuring equipment for gas and water phase. The ozone generated from atmospheric oxygen inside the generator is injected into the tubular reactor via the inlet nozzle. The reactor has a high internal recirculation rate, which results in a fast transition of the ozone from the gas to the liquid phase. The residual gas is removed from the system via a gas separator.

A schematic flow diagram of the examined unit configuration is shown in Figure 2. The influent of the plant was continuously filtered (50 μm). Via a 3-way valve and magnetic-inductive flowmeter (MID) measurement (IFM SM6100), the feed volume was controlled. The feed volume flow is first led into the photocatalytic reactor, whose individual cascades are

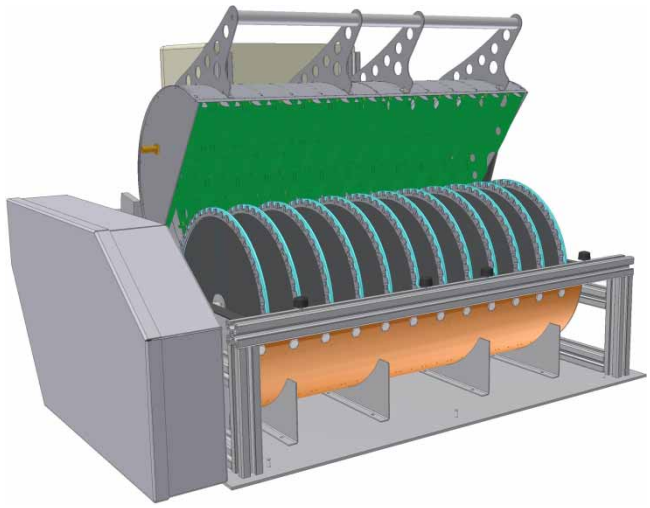

Figure 1 | Three-dimensional model of the photocatalytic immersion body reactor (© Lynatox GmbH, 2020).

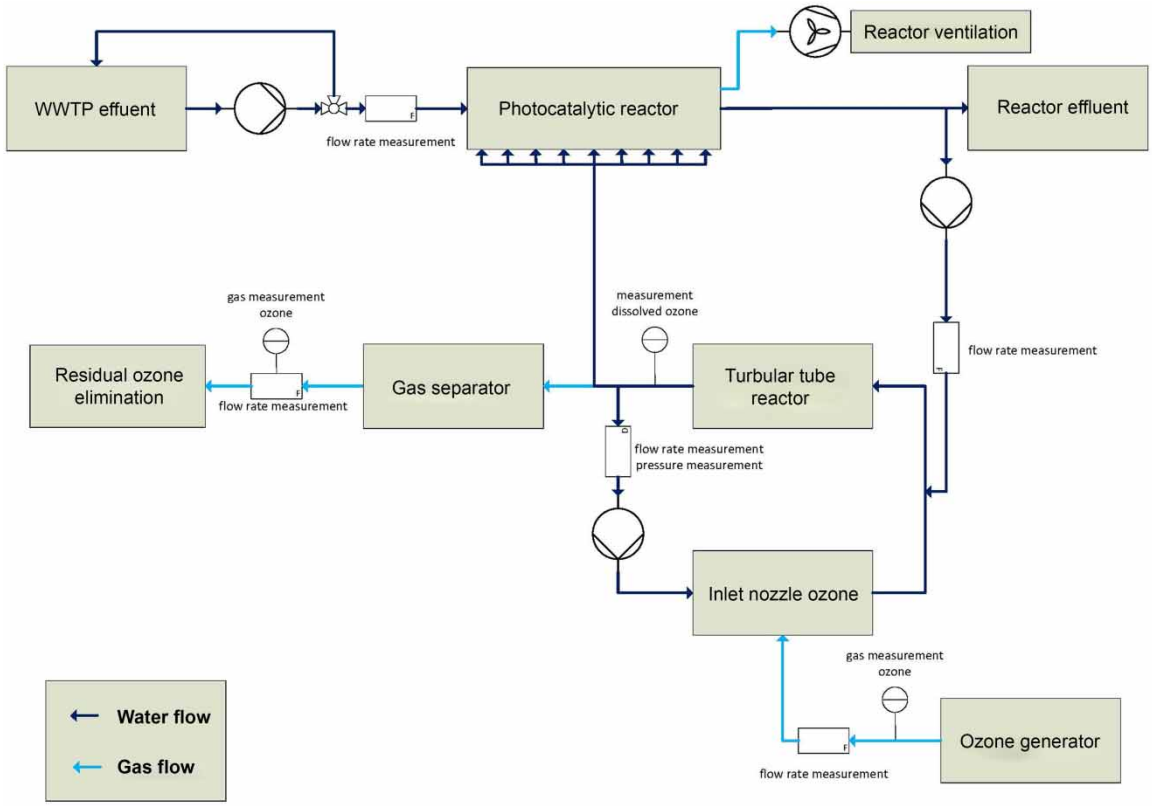

Figure 2 | Flow diagram of the photocatalytic reactor and the ozonation unit.

flowed through in series. A portion of the reactor effluent is fed to the ozonation system via a membrane pump. Here, a dissolved ozone concentration of 6.5 mg/l was set by means of a measuring electrode. This ozone enriched water is dosed equally distributed into all cascades of the photocatalysis via a distribution device, whereby a control of the feed quantity was also carried out via MID measurement (IFM SM6100).

Before starting the experiment, the reactor volume of the photocatalytic reactor was initially replaced with fresh effluent from the wastewater treatment plant once. Subsequently, the respective operating parameters were set. After an operating time of at least 90 minutes (approximately. 1.5 times the hydraulic retention time of the photocatalytic reactor), the reactor feed and operation were stopped simultaneously. This was followed by taking samples from reactor feed and from six cascades of the photocatalytic reactor. The samples were stored cooled and dark until analysis. The analysis was carried out at a maximum of 14 days after sampling. The experimental program was divided into three main steps:

- measurement of the degradation efficiency by photocatalysis
- measurement of the degradation efficiency by ozonation
- measurement of the degradation efficiency by photocatalytic ozonation.

The degradation efficiency of the photocatalysis alone (without ozonation) was investigated under variation of the electrical LED power for the irradiances 50, 100 and 150 W/m^2. The ozonation alone was measured for DOC-related doses of 0.2, 0.4, 0.6 mg O_3/mg DOC. The used ozone doses correspond in maximum to the current recommendations for ozonation processes as a fourth treatment stage in Germany (Gottschalk *et al.* 2010; Fleiner *et al.* 2015). The application of photocatalytic ozonation was investigated for the combinations of area-related irradiation powers of 25, 50 and 100 W/m^2 and specific ozone doses of 0.2, 0.4 and 0.6 mg O_3/mg DOC. An overview of the experimental parameters used is given in Table 1.

Analytical methods

The chemical analysis of the trace substances was carried out using liquid chromatography tandem mass spectrometry (LC-MS/MS) analogous to previous publications (Schnabel *et al.* 2020). The used high performance liquid chromatography (HPLC) was a

Table 1 | Experimental parameters

Number	LED power [W/m^2]	Ozone dose [mg O_3/mg DOC]
1.1	50	–
1.2	100	–
1.3	150	–
2.1	–	0.2
2.2	–	0.4
2.3	–	0.6
3.1	25	0.2
3.2	25	0.4
3.3	25	0.6
3.4	50	0.2
3.5	50	0.4
3.6	50	0.6
3.7	100	0.2
3.8	100	0.4
3.9	100	0.6

Dionex R3000 system with gradient pump and autosampler. The HPLC eluent was ultrapure water with 1 mmol/l ammonium acetate and acetonitrile with 0.1% acetic acid. A Phenomenex Synergi 2.5 µm hydro PP column measuring 100 × 2 mm was used as the analytical separation column. The flow rate was 0.25 ml/min and the gradient was run from 4% acetonitrile to 96% acetonitrile in 28 minutes. The injection volume was a 100 µl sample, which was mixed with 10 µl internal standard. For detection, a Sciex API 4000 triple quadrupole mass spectrometer with electro-spray ionization was used. For each substance two multiple reaction monitoring mass transitions were evaluated. The following substances were analyzed within this work: amisulpride, benzotriazole, candesartan, carbamazepine, diclofenac, gabapentin, 1-methylbenzotriazole and metoprolol. The DOC was measured with a Multi N/C analyzer from Analytik Jena. The inorganic carbon was removed from 5 ml of sample by blowing out with oxygen after the addition of 100 µl of 1 molar hydrochloric acid. During the measurement, a control determination of the inorganic carbon was carried out by adding phosphoric acid. The organic carbon was determined after catalytic combustion of a 1 ml sample solution in the oxygen stream at 800 °C on a platinum catalyst. The carbon dioxide formed was detected by non-dispersive near infrared spectroscopy. Calibration of the measurement system was performed equidistantly with 10 points between 1 and 10 mg/l using potassium hydrogen phthalate solutions. Blank values and control standards were measured regularly as quality assurance measures. All analytical measurements were carried out in duplicate.

Kinetic and modelling

According to (Lin *et al.* 2009; Asenjo *et al.* 2013) the kinetic of photocatalytic degradation follows the Langmuir–Hinshelwood (L-H) model. The L-H model reaction rate can be calculated using Equation (10):

$$r = -\frac{dC}{dt} = k_{LH}\frac{K_L C_p}{1 + K_L C_p} \tag{10}$$

where r is the reaction rate, k_{LH} is the specific rate constant, K_L is the Langmuir constant and C_p the liquid concentration. For the application of the L-H model in photocatalytic treatment of real wastewater matrices the presence of reaction products and no related substances must be considered by adding a modified adsorption term (Equation 11):

$$r = -\frac{dC}{dt} = k_{LH}\frac{K_L C_p}{1 + K_L C_p + \sum_{i=1}^{n} K_i C_i (i = 1, n)} \tag{11}$$

where K_i and C_i are the adsorption constant and concentration of every contained substance at any given time. However in real wastewater samples only summative measurements are possible (e.g. TOC, COD). At low substance concentration, which applies for micro-pollutants in most wastewater treatment plant effluents, the term $1 + K_L C_p + \sum_{i=1}^{n} K_i C_i (i = 1, n)$ can be neglected and the reaction follows a pseudo-first-order decay rate as described below (Equation 12):

$$r = -\frac{dC}{dt} = k_{LH} K_L C_p = k C_p \tag{12}$$

For photocatalytic ozonation, adsorption-independent reaction pathways must be amended with direct oxidation by ozone and the reaction of radicals in the liquid phase. By (Mehrjouei *et al.* 2015) the following formula is presented (Equation 13):

$$r = -\frac{dC}{dt} = k_{O_3} C_{O_3} C_p + k_{OH} C_{OH} C_p + k_{LH} \frac{K_L C_p}{1 + K_L C_{eq}} \tag{13}$$

where C_{O_3} and C_{OH} represent the ozone and hydroxyl radical concentrations in water and k_{O_3} and k_{OH} the corresponding reaction constants. Here, in addition to hydroxyl radicals, the reactions of other reactants are also summarized under these reaction rates (Mehrjouei *et al.* 2015). In the context of this work, as a measurement of concentrations for ozone and radicals in the water phase was not possible, Equation (14) was simplified on the basis of Equation (12), resulting in first-order kinetics:

$$r = -\frac{dC}{dt} = k_{O_3} C_{O_3} C_p + k_{OH} C_{OH} C_p + k_{LH} K_L C_p = (k_{O_3} C_{O_3} + k_{OH} C_{OH} + k_{LH} K_L) C_p = k C_p \tag{14}$$

To ensure better interpretability of the kinetic parameters, calculated degradation constants were converted to half-lives according to Equation (15):

$$T_{1/2} = \frac{\ln 2}{k} \tag{15}$$

Due to the series connection of the individual cascades of the photocatalytic reactor, the behavior of the system under consideration approximates a plug flow reactor. Within the evaluation, hydraulic residence times were therefore equated with the number of cascades flowing through. A total residence time of 60 minutes and six sampled individual cascades results in time intervals of 10 minutes. The underlying decay constant k was determined from the measured concentration curves via exponential parameter fit using the following equation:

$$y = A1 * \exp\left(-\frac{(x - x0)}{t1}\right) \tag{16}$$

Figure 3 shows an exemplary illustration of the concentration curves including the respective parameter fits for carbamazepine and diclofenac. Carbamazepine shows a behavior similar to the other micro-pollutants investigated, while diclofenac is marked by elevated reaction rates. For photocatalysis as well as photocatalytic ozonation, the first-order reaction rates reported by many authors could also be confirmed for this application in real wastewater matrix (Gaya & Abdullah 2008; Mehrjouei *et al.* 2015; Kanakaraju *et al.* 2018; Mecha & Chollom 2020). Due to fluctuating feed concentrations during the operating time of individual experimental steps, small concentration fluctuations occurred within the reactor in individual cases. For this reason, the parameter fit was performed using parameter $A1$. The time variance of the feed is compensated while the concentration-independent exponential time curve can be correctly captured by the parameter $t1$.

The reaction of ozone in wastewater does not follow first-order kinetics due to a successive consumption of the reactant ozone (Sonntag & Gunten 2012). Due to the high reaction rate of ozone and the sub-stoichiometric dosing used, it can be assumed that ozone reacts completely within each cascade. Therefore, the evaluation of the reaction behavior of ozone is performed using the well known correlation between DOC-related ozone amount and the degradation rate of micro-pollutants (Rice 1996; Gottschalk *et al.* 2010). All measured concentrations, as well as the corresponding half-lives and fitting parameters, are shown in the appendix.

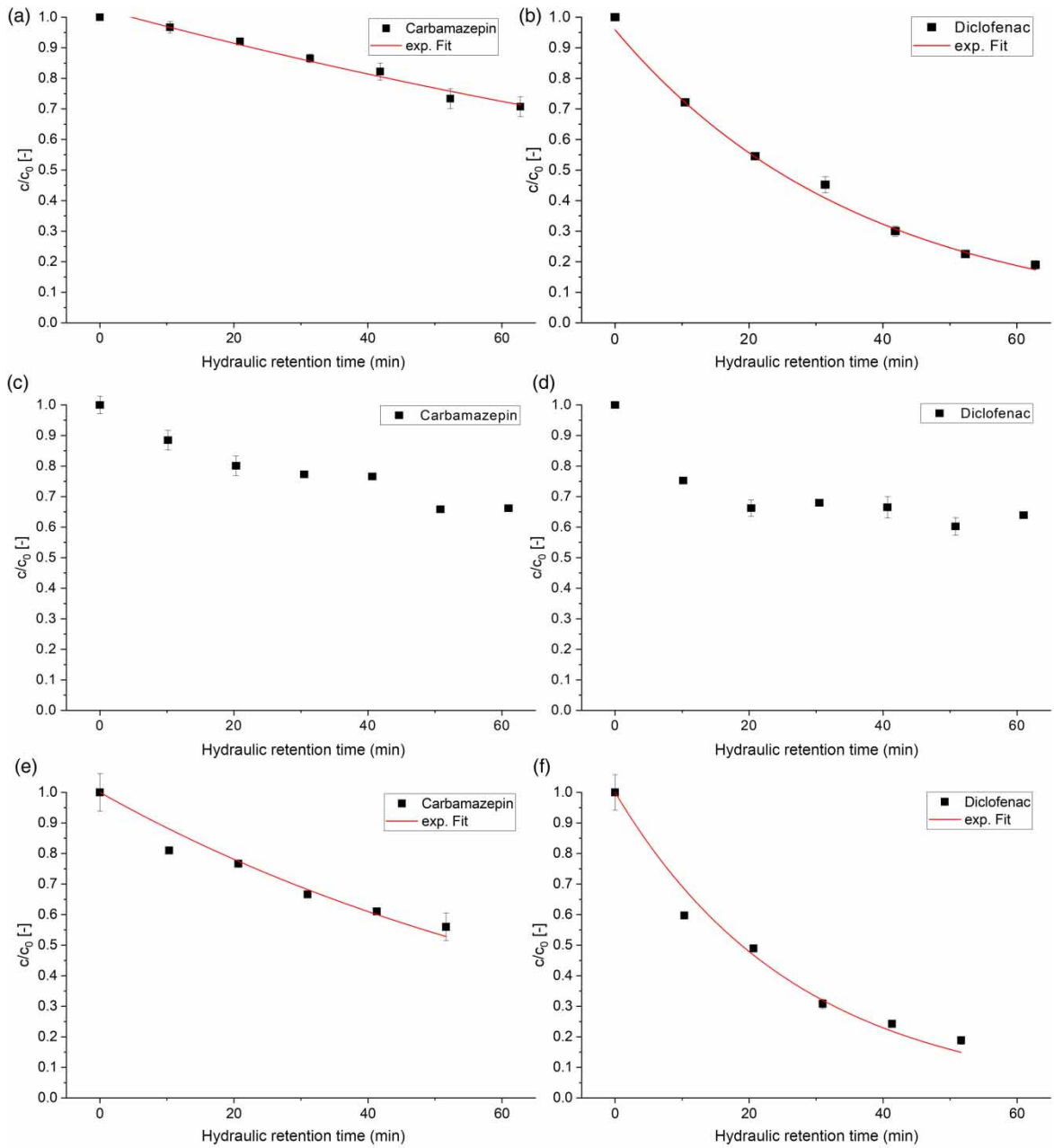

Figure 3 | Exemplary illustration of the observed degradation kinetics for photocatalysis (1 + 2), ozonation (3 + 4) and photocatalytic ozonation (5 + 6).

RESULTS

The measured influent concentrations of the unit are shown in Figure 4. There were high loads of benzotriazole, diclofenac and gabapentin in particular in the wastewater treatment plant effluent. Amisulpride had the lowest concentration with a value range of 200–650 ng/l. High fluctuations in the measured concentrations of almost all micro-pollutants are evident. Benzotriazole shows the highest fluctuation with an amplitude of 4,700 ng/l. These concentration fluctuations also occur at successive investigation steps, i.e. at time intervals of 2–3 hours.

Figure 5 shows the half-life values of a purely photocatalytic treatment under variable irradiance. Of all the micro-pollutants considered, diclofenac shows the greatest affinity for photocatalytic degradation with half-lives of 17–28 minutes. The other

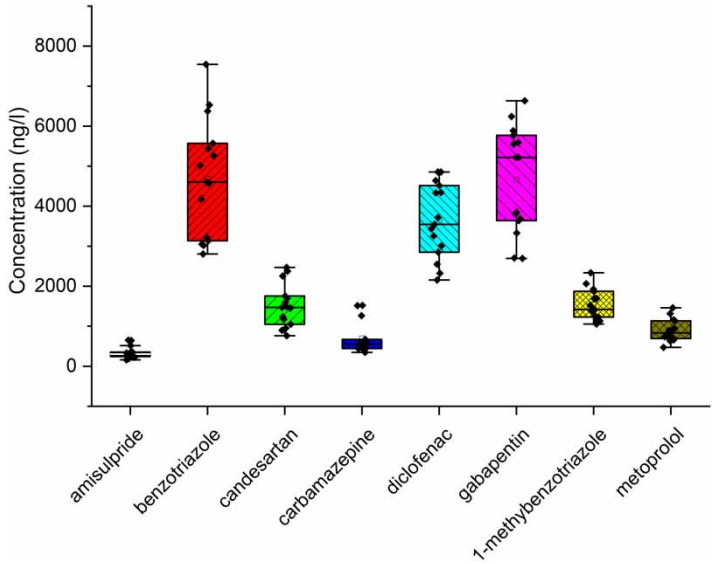

Figure 4 | Concentrations of micro-pollutants in the wastewater treatment plant effluent of Weimar Tiefurt.

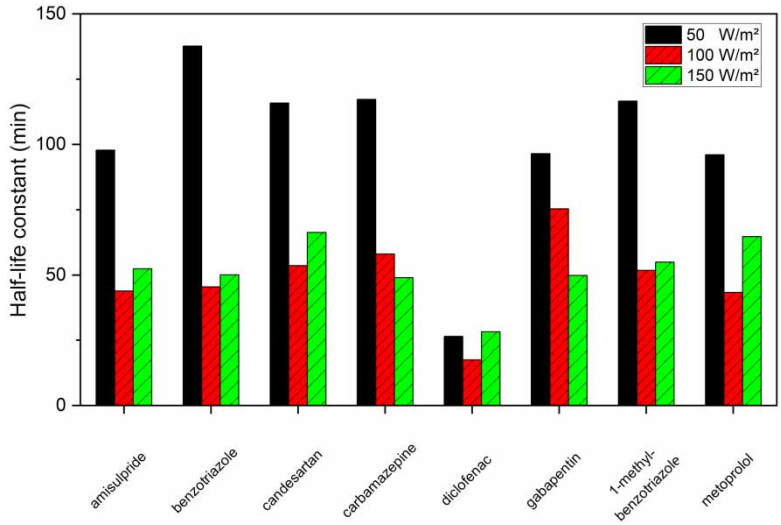

Figure 5 | Half-live constants for photocatalytic degradation with different electrical irradiation energy per base surface.

substances studied for irradiances of 100–150 W/m^2 have similar half-lives of 40–60 minutes. For irradiances of 50 W/m^2, all micro-pollutants, with the exception of diclofenac, show a significant reduction in the reaction rate with half-lives of 96–138 minutes. This reduction of the reaction rate therefore shows a substance-dependent behavior, while the approximation of a maximum reaction rate with increasing irradiance occurs analogously for most micro-pollutants.

The degradation rates achieved within the reactor system with variable DOC-related ozone dosage are shown in Figure 6. Here, the known relationship between ozone dose and degradation rate is generally confirmed. Gabapentin shows a deviating behavior in this case. Furthermore, it becomes evident that degradation rates achievable by ozone alone are substance-specific.

The combined use of ozone and photocatalysis within the reactor can increase the reaction rates for all the micro-pollutants studied, as shown in Figure 7. For example, half-lives are reduced by 50% at ozone doses of 0.4–0.6 mg O_3/mg DOC for amisulpride, benzotriazole, candesartan, carbamazepine, and 1-methylbenoztiazole. Smaller effects were found for diclofenac

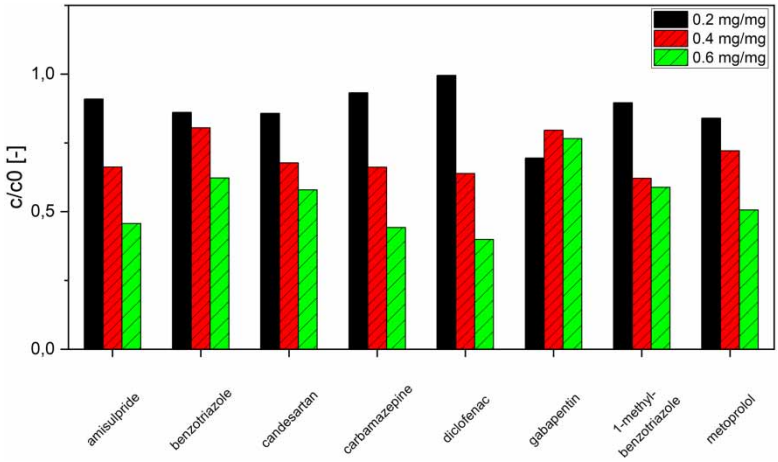

Figure 6 | Micro-pollutant degradation rate in the reactor effluent for different ozone doses within the reactor.

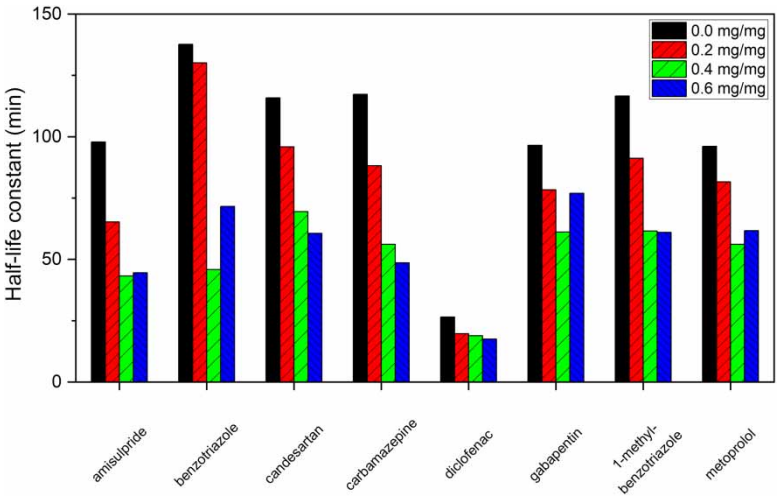

Figure 7 | Half-live constants for micro-pollutant degradation via photocatalysis and photocatalytic ozonation with different ozone doses and 50 W/m^2 electrical irradiation energy per base surface.

and gabapentin. It is further shown that increasing the ozone dose beyond 0.4 mg O_3/mg DOC for an irradiance of 50 W/m^2 does not lead to any further increase in the reaction rate

For the lowest irradiance tested of 25 W/m^2, there is a clear effect of the ozone dose on the half-lives of the micro-pollutants (see Figure 8). For ozone doses of 0.2 mg O_3/mg DOC, half-lives of about 100–170 minutes are achieved, with the exception of diclofenac. Increasing the ozone dose to 0.4 mg O_3/mg DOC can reduce these to 40–60 minutes. A further increase of the ozone dose does not cause a further reduction of the half-life, analogously to 50 W/m^2 irradiance.

Figure 9 shows the measured half-lives within a combined application of 0.4 mg O_3/mg DOC and variable irradiance. It is apparent that increasing the irradiance from 50 to 100 W/m^2 does not lead to any increase in the reaction rate. A reduction of the irradiance from 50 to 25 W/m^2 does not lead to a reduction of the reaction rate with the exception of amisulpride and gabapentin.

Rivas *et al.* (2012) using synthetic mixtures of pharmaceuticals in ultrapure water, achieved half-lives of approximately 10–20 minutes for diclofenac and 10–50 minutes for metoprolol using a solely photocatalytic application with variable concentrations of suspended titanium dioxide. For an application as photocatalytic ozonation, a 50% TOC decrease was achieved after 30 minutes compared to 80 minutes for a photocatalytic application alone. The reactor volume-related

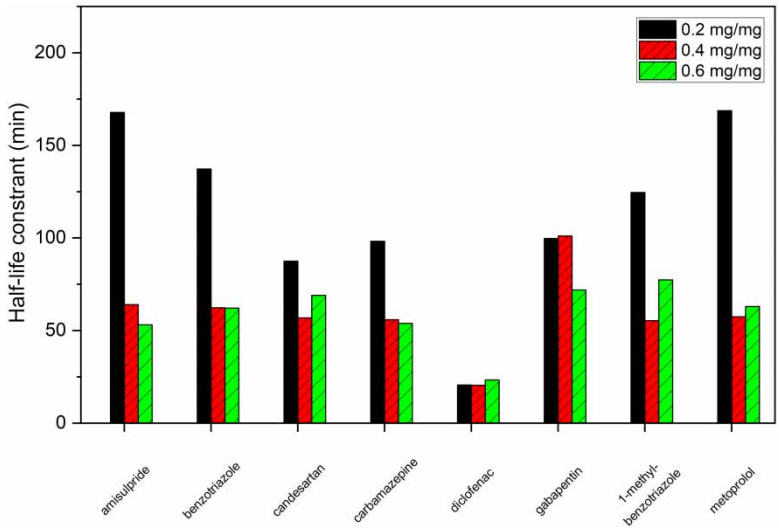

Figure 8 | Half-live constants for micro-pollutant degradation via photocatalytic ozonation with different ozone doses and 25 W/m^2 electrical irradiation energy per base surface.

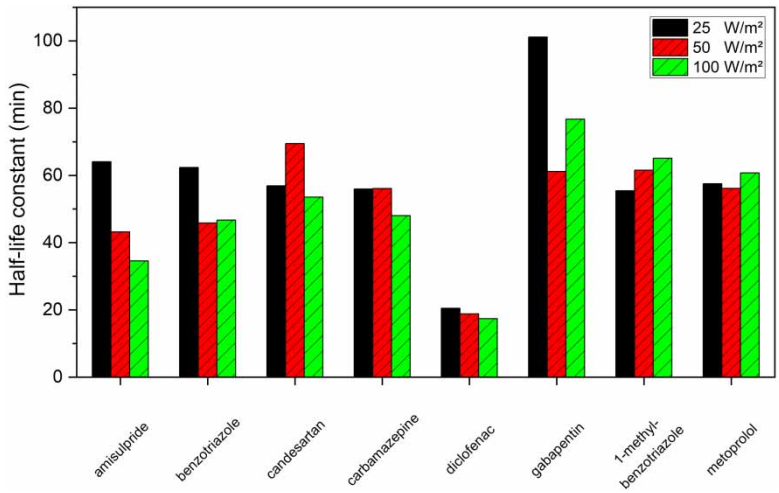

Figure 9 | Half-live constants micro-pollutant degradation via photocatalytic ozonation with different electrical irradiation energy per base surface and a specific ozone dose of 0.4 mg O_3/mg DOC.

electrical radiation power was 700 W/l here. Within the system studied, this was approximately 3–14 W/l, although efficiency differences between high pressure mercury lamps and LEDs must be considered here. In Aguinaco *et al.* (2012), a 90% TOC of a diclofenac ultrapure water solution was achieved after 15 minutes. In ultrapure water, 50% degradation of the parent compound diclofenac was achieved after 1–3 minutes for photocatalysis and photocatalytic ozonation using particulate titanium dioxide. The ozone doses used here were in the range of 0–30 mg/l. In experiments using secondary effluent, 50% degradation was achieved after 0.5–1 minute. The specific ozone dose here was approximately. 0.2 mg/mg after 1 minute. Unfortunately, a measurement of the sole reaction rate of ozone was not carried out in this source. Within this work, half-lives of 17–20 minutes were achieved for diclofenac. However, the ozone dosage is done per reactor cascade, so that after 20 minutes only one-third of the ozone dose (e.g. 0.066 mg/mg) was added. The existing findings of previous laboratory tests could be essentially confirmed. Overall, compared to existing literature, a lower degradation rate was

observed within the carrier-bound reactor studied, with the slower addition of ozone exerting a significant influence. Direct comparability of reactor systems and reaction rates is difficult due to the influences of real wastewater constituents on the respective reaction rates of micro-pollutants, different operating parameters and lack of measurement data within existing literature.

CONCLUSIONS

The objective of this work was to prove the suitability of photocatalytic ozonation by means of a photocatalytic immersion rotary body reactor and a substream ozonation as a 4th cleaning stage for the application within real wastewater. By varying the essential operating parameters electrical irradiation power and ozone dose, a first optimization approach was given. By photocatalysis as well as by photocatalytic ozonation a significant degradation of all investigated substances was achieved. A maximum substance-specific reaction rate of the reactor system was measured, which could not be influenced either by increasing the irradiation power or the ozone dose. By operating the reactor as a photocatalytic ozonation system, electrical irradiation power could be reduced by up to 75% at ozone doses of 0.4 mg O_3/mg DOC at the same reaction rates. At 100 W/m^2 and a retention time of one hour, the energy demand of the LEDs relative to the wastewater volume would be 9.76 kWh/m^3. Photocatalytic ozonation can achieve similar reaction rates at 25 W/m^2, which corresponds to a wastewater volume-related energy requirement of 2.44 kWh/m^3 for the same treatment duration. With photocatalytic ozonation desired radical concentration can be formed using lower levels of UV-A radiation, which enables more efficient use of existing radiation potentials and/or energy resources. Within the reactor set-up used, it was not possible to investigate this effect for lower irradiation powers, so further potential electrical energy savings are possible. The approximation of the measured reaction rates to a maximum value indicates a limitation of this reactor type independent of radical concentrations. The degradation of micro-pollutants by photocatalysis and photocatalytic ozonation within an immersion rotary body reactor is also influenced by adsorption and diffusion in addition to the radical concentrations. The concentrations of generated radicals can be influenced by photon flux and ozone dosage. The assumption is that a major limitation for this reactors degradations speed is the layer thickness of water on the cyclically wetted rotating disks. Under this assumption, further limitation of reaction rates are to be expected through further scale-up processes towards large-scale application. For upcoming studies, a consideration of cleaning performance for permanently submerged reactor systems using similar process parameters is recommended.

DATA AVAILABILITY STATEMENT

All relevant data are included in the paper or its Supplementary Information.

REFERENCES

Abegglen, C. & Siegrist, H. 2012 *Mikroverunreinigungen aus kommunalem Abwasser Verfahren zur weitergehenden Elimination auf Kläranlagen (Micropollutants From Municipal Wastewater Process for Further Elimination in Sewage Treatment Plants)*. Federal Office for the Environment BAFU.

Aemig, Q., Hélias, A. & Patureau, D. 2021 Impact assessment of a large panel of organic and inorganic micropollutants released by wastewater treatment plants at the scale of France. *Water Research* **188**, 116524. doi: 10.1016/j.watres.2020.116524.

Aguinaco, A., Beltrán, F. J., García-Araya, J. F. & Oropesa, A. 2012 Photocatalytic ozonation to remove the pharmaceutical diclofenac from water: influence of variables. *Chemical Engineering Journal* **189–190**, 275–282.

Asenjo, N. G., Santamaría, R., Blanco, C., Granda, M., Álvarez, P. & Menéndez, R. 2013 Correct use of the Langmuir–Hinshelwood equation for proving the absence of a synergy effect in the photocatalytic degradation of phenol on a suspended mixture of titania and activated carbon. *Carbon* **55**, 62–69.

Augustina, T. E., Ang, H. M. & Vareek, V. K. 2005 A review of synergistic effect of photocatalysis and ozonation on wastewater treatment. *Journal of Photochemistry and Photobiology C: Photochemistry Reviews* **6** (6), 264–273.

Bourgin, M., Beck, B., Boehler, M., Borowska, E., Fleiner, J., Salhi, E., Teichler, R., von Gunten, U., Siegrist, H. & McArdell, C. S. 2018 Evaluation of a full-scale wastewater treatment plant upgraded with ozonation and biological post-treatments: abatement of micropollutants, formation of transformation products and oxidation by-products. *Water Research* **129**, 486–498. doi: 10.1016/j.watres.2017.10.036.

Chávez, A. M., Ribeiro, A. R., Moreira, N. F. F., Silva, A. M. T., Rey, A., Álvarez, P. M. & Beltrán, F. J. 2019 Removal of organic micropollutants from a municipal wastewater secondary effluent by UVA-LED photocatalytic ozonation. *Catalysts* **9** (5), 472. doi: 10.3390/catal9050472.

Fleiner, J., Siegrist, H., Böhler, M., McAdell, C., Teichler, R., Bourgin, M. & Schachtler, 2015 *Ozonung ARA Neugut, Dübendorf – Grosstechnische Optimierung der Ozondosierung (Ozonation ARA Neugut, Dübendorf – Large-Scale Optimization of the Ozone Dosing System)*. Federal Office for the Environment BAFU.

Garrido-Cardenas, J. A., Esteban-García, B., Agüera, A., Sánchez-Pérez, J. A. & Manzano-Agugliaro, F. 2019 Wastewater treatment by advanced oxidation process and their worldwide research trends. *International Journal of Environmental Research and Public Health* **17** (1). doi: 10.3390/ijerph17010170.

Gaya, U. I. & Abdullah, A. H. 2008 Heterogeneous photocatalytic degradation of organic contaminants over titanium dioxide: a review of fundamentals, progress and problems. *Journal of Photochemistry and Photobiology C: Photochemistry Reviews* **9** (1), 1–12. doi: 10.1016/j.jphotochemrev.2007.12.003.

Gimeno, O., Rivas, F. J., Beltrán, F. J. & Carbajo, M. 2007 Photocatalytic ozonation of winery wastewaters. *Journal of Agricultural and Food Chemistry* **55** (24), 9944–9950.

Gottschalk, C., Libra, J. & Saupe, A. 2010 *Ozonation of Water and Wastewater. A Practical Guide to Understanding Ozone and its Applications*. WILEY-VCH Verlag GmbH & Co. KGaA, Weinheim.

GSchV 2020 *Gewässerschutzverordnung* (Water Protection Ordinance) Switzerland. 1 January 2020.

Guillossou, R., Le Roux, J., Mailler, R., Vulliet, E., Morlay, C., Nauleau, F., Gasperi, J. & Rocher, V. 2019 Organic micropollutants in a large wastewater treatment plant: what are the benefits of an advanced treatment by activated carbon adsorption in comparison to conventional treatment? *Chemosphere* **218**, 1050–1060. doi: 10.1016/j.chemosphere.2018.11.182.

Guillossou, R., Le Roux, J., Brosillon, S., Mailler, R., Vulliet, E., Morlay, C., Nauleau, F., Rocher, V. & Gaspéri, J. 2020 Benefits of ozonation before activated carbon adsorption for the removal of organic micropollutants from wastewater effluents. *Chemosphere* **245**, 125530. doi: 10.1016/j.chemosphere.2019.125530.

Hassan, G. K., Gad-Allah, T. A., Badawy, M. I. & El-Gohary, F. A. 2021 Remediation of ammonia-stripped sanitary landfill leachate by integrated heterogeneous Fenton process and aerobic biological methods. *International Journal of Environmental Analytical Chemistry*, 1–14. doi: 10.1080/03067319.2021.1969381.

Kanakaraju, D., Glass, B. D. & Oelgemöller, M. 2018 Advanced oxidation process-mediated removal of pharmaceuticals from water: a review. *Journal of Environmental Management* **219**, 189–207.

Kanaujiya, D. K., Paul, T., Sinharoy, A. & Pakshirajan, K. 2019 Biological treatment processes for the removal of organic micropollutants from wastewater: a review. *Current Pollution Reports* **5** (3), 112–128. doi: 10.1007/s40726-019-00110-x.

Kang, W., Chen, S., Yu, H., Xu, T., Wu, S., Wang, X., Lu, N., Quan, X. & Liang, H. 2021 Photocatalytic ozonation of organic pollutants in wastewater using a flowing through reactor. *Journal of Hazardous Materials* **405**, 124277. doi: 10.1016/j.jhazmat.2020.124277.

Kisch, H. 2015 Semiconductor Photocatalysis – Principles and Applications: Wiley VCH.

Lin, Y., Ferronato, C., Deng, N., Wu, F. & Chovelon, J.-M. 2009 Photocatalytic degradation of methylparaben by TiO2: multivariable experimental design and mechanism. *Applied Catalysis B: Environmental* **88** (1–2), 32–41.

Mecha, A. C. & Chollom, M. N. 2020 Photocatalytic ozonation of wastewater: a review. *Environmental Chemistry Letters* **18** (5), 1491–1507.

Mehrjouei, M., Müller, S. & Möller, D. 2012 Synergistic effect of the combination of immobilized TiO2, UVA and ozone on the decomposition of dichloroacetic acid. *Journal of Environmental Science and Health. Part A, Toxic/Hazardous Substances & Environmental Engineering* **47** (8), 1073–1081.

Mehrjouei, M., Müller, S. & Möller, D. 2015 A review on photocatalytic ozonation used for the treatment of water and wastewater. *Chemical Engineering Journal* **263**, 209–219. doi: 10.1016/j.cej.2014.10.112.

Mena, E., Rey, A., Acedo, B., Beltrán, F. J. & Malato, S. 2012 On ozone-photocatalysis synergism in black-light induced reactions: oxidizing species production in photocatalytic ozonation versus heterogeneous photocatalysis. *Chemical Engineering Journal* **204–206**, 131–140. doi: 10.1016/j.cej.2012.07.076.

Pichat, P., Cermenati, L., Albini, A., Mas, D., Delprat, H. & Guillard, C. 2000 Degradation processes of organic compounds over UV-irradiated TiO_2. Effect of ozone. *Research on Chemical Intermediates* **26** (2), 161–170. doi: 10.1163/156856700X00200.

Rice, R. G. 1996 Applications of ozone for industrial wastewater treatment – a review. *Ozone: Science & Engineering* **18** (6), 477–515. doi: 10.1080/01919512.1997.10382859.

Rivas, F. J., Beltrán, F. J. & Encinas, A. 2012 Removal of emergent contaminants: integration of ozone and photocatalysis. *Journal of Environmental Management* **100**, 10–15.

Rodríguez, E. M., Márquez, G., León, E. A., Álvarez, P. M., Amat, A. M. & Beltrán, F. J. 2013 Mechanism considerations for photocatalytic oxidation, ozonation and photocatalytic ozonation of some pharmaceutical compounds in water. *Journal of Environmental Management* **127**, 114–124.

Santiago-Morales, J., Gómez, M. J., Herrera, S., Fernández-Alba, A. R., García-Calvo, E. & Rosal, R. 2012 Oxidative and photochemical processes for the removal of galaxolide and tonalide from wastewater. *Water Research* **46** (14), 4435–4447. doi: 10.1016/j.watres.2012.05.051.

Schnabel, T., Mehling, S., Londong, J. & Springer, C. 2020 Hydrogen peroxide-assisted photocatalytic water treatment for the removal of anthropogenic trace substances from the effluent of wastewater treatment plants. *Water Science and Technology*. doi: 10.2166/wst.2020.481.

Schnabel, T., Jautzus, N., Mehling, S., Springer, C. & Londong, J. 2021 Photocatalytic degradation of hydrocarbons and methylene blue using floatable titanium dioxide catalysts in contaminated water. *Journal of Water Reuse and Desalination* **11** (2), 224–235. doi: 10.2166/wrd.2021.118.

Sillanpää, M., Ncibi, M. C. & Matilainen, A. 2018 Advanced oxidation processes for the removal of natural organic matter from drinking water sources: a comprehensive review. *Journal of Environmental Management* **208**, 56–76. doi: 10.1016/j.jenvman.2017.12.009.

Sonntag, C. v. & Gunten, U. v. 2012 *Chemistry of Ozone in Water and Wastewater Treatment. From Basic Principles to Applications*. IWA Publishing, London.

Weber, F.-A., Bergmann, A., Beek, T. a. d., Carius, A. & Grüttner, G. 2014 *Pharmaceuticals in the Environment – the Global Perspective Occurrence, Effects, and Potential Cooperative Action Under SAICM*. Federal Environment Agency (UBA), Dessau-Roßlau, Germany.

Xiao, J., Xie, Y., Rabeah, J., Brückner, A. & Cao, H. 2020 Visible-light photocatalytic ozonation using graphitic C_3N_4 catalysts: a hydroxyl radical manufacturer for wastewater treatment. *Accounts of Chemical Research* **53** (5), 1024–1033. doi: 10.1021/acs.accounts.9b00624.

First received 29 September 2021; accepted in revised form 29 November 2021. Available online 10 December 2021